

Observation of  
viscosity transition in  
 $\alpha$ -pinene secondary  
organic aerosol

E. Järvinen et al.

This discussion paper is/has been under review for the journal Atmospheric Chemistry and Physics (ACP). Please refer to the corresponding final paper in ACP if available.

# Observation of viscosity transition in $\alpha$ -pinene secondary organic aerosol

E. Järvinen<sup>1</sup>, K. Ignatius<sup>2</sup>, L. Nichman<sup>3</sup>, T. B. Kristensen<sup>2</sup>, C. Fuchs<sup>4</sup>, N. Höppel<sup>1</sup>, J. C. Corbin<sup>4</sup>, J. Craven<sup>5</sup>, J. Duplissy<sup>6</sup>, S. Ehrhart<sup>7</sup>, I. El Haddad<sup>4</sup>, C. Frege<sup>4</sup>, S. J. Gates<sup>4</sup>, H. Gordon<sup>7</sup>, C. R. Hoyle<sup>4,8</sup>, T. Jokinen<sup>6</sup>, P. Kallinger<sup>9</sup>, J. Kirkby<sup>7,10</sup>, A. Kiselev<sup>1</sup>, K.-H. Naumann<sup>1</sup>, T. Petäjä<sup>6</sup>, T. Pinterich<sup>9</sup>, A. S. H. Prevot<sup>4</sup>, H. Saathoff<sup>1</sup>, T. Schiebel<sup>1</sup>, K. Sengupta<sup>11</sup>, M. Simon<sup>10</sup>, J. Tröstl<sup>4</sup>, A. Virtanen<sup>12</sup>, P. Vochezer<sup>1</sup>, S. Vogt<sup>1</sup>, A. C. Wagner<sup>10</sup>, R. Wagner<sup>1</sup>, C. Williamson<sup>10,13,14</sup>, P. M. Winkler<sup>9</sup>, C. Yan<sup>6</sup>, U. Baltensperger<sup>4</sup>, N. M. Donahue<sup>15</sup>, R. C. Flagan<sup>16</sup>, M. Gallagher<sup>3</sup>, A. Hansel<sup>17</sup>, M. Kulmala<sup>6</sup>, F. Stratmann<sup>2</sup>, D. R. Worsnop<sup>18</sup>, O. Möhler<sup>1</sup>, T. Leisner<sup>1</sup>, and M. Schnaiter<sup>1</sup>

<sup>1</sup>Karlsruhe Institute of Technology, Institute for Meteorology and Climate Research, P.O. Box 3640, 76021 Karlsruhe, Germany

<sup>2</sup>Institute for Tropospheric Research (TROPOS), 04318 Leipzig, Germany

<sup>3</sup>School of Earth, Atmospheric and Environmental Sciences, University of Manchester, Manchester, M13 9PL, UK

<sup>4</sup>Laboratory of Atmospheric Chemistry, Paul Scherrer Institute, Villigen, Switzerland

<sup>5</sup>California institute of technology, department of chemical engineering, Pasadena, CA, 91125, USA

Title Page

Abstract Introduction

Conclusions References

Tables Figures

◀ ▶

◀ ▶

Back Close

Full Screen / Esc

Printer-friendly Version

Interactive Discussion



<sup>6</sup>Helsinki Institute of Physics and University of Helsinki, Department of Physics, Helsinki, Finland

<sup>7</sup>CERN, 1211, Geneva, Switzerland

<sup>8</sup>Swiss Federal Institute for Forest Snow and Landscape Research (WSL)-Institute for Snow and Avalanche Research (SLF), 7270 Davos, Switzerland

<sup>9</sup>Faculty of Physics, University of Vienna, Austria

<sup>10</sup>Institute for Atmospheric and Environmental Sciences, Goethe-University Frankfurt am Main, Campus Riedberg Altenhöferallee 1, 60438 Frankfurt am Main, Germany

<sup>11</sup>University of Leeds, School of Earth and Environment, LS2-9JT Leeds, UK

<sup>12</sup>Department of Applied Physics, University of Eastern Finland, Kuopio, Finland

<sup>13</sup>NOAA Earth Systems Research Laboratory (ESRL), Chemical Sciences Division, 325 Broadway, Boulder, Colorado 80305, USA

<sup>14</sup>Cooperative Institute for Research in Environmental Sciences (CIRES), University of Colorado Boulder, UCB 216, Boulder, Colorado 80309, USA

<sup>15</sup>Center for Atmospheric Particle Studies, Carnegie Mellon University, 5000 Forbes Ave., Pittsburgh PA 15213, USA

<sup>16</sup>California Institute of Technology, Division of Chemistry and Chemical Engineering, Pasadena, California 91125, USA

<sup>17</sup>Institute for Ion and Applied Physics, 6020 Innsbruck and Ionicon Analytik GmbH, 6020 Innsbruck, Austria

<sup>18</sup>Aerodyne Research, Inc., Billerica, MA 08121, USA

Received: 4 September 2015 – Accepted: 2 October 2015 – Published: 22 October 2015

Correspondence to: E. Järvinen (emma.jaervinen@kit.edu)

Published by Copernicus Publications on behalf of the European Geosciences Union.

Observation of  
viscosity transition in  
 $\alpha$ -pinene secondary  
organic aerosol

E. Järvinen et al.

Title Page

Abstract

Introduction

Conclusions

References

Tables

Figures



Back

Close

Full Screen / Esc

Printer-friendly Version

Interactive Discussion



## Abstract

Under certain conditions, secondary organic aerosol (SOA) particles can exist in the atmosphere in an amorphous solid or semi-solid state. To determine their relevance to processes such as ice nucleation or chemistry occurring within particles requires knowledge of the temperature and relative humidity (RH) range for SOA to exist in these states. In the CLOUD experiment at CERN, we deployed a new in-situ optical method to detect the viscosity of  $\alpha$ -pinene SOA particles and measured their transition from the amorphous viscous to liquid state. The method is based on the depolarising properties of laboratory-produced non-spherical SOA particles and their transformation to non-depolarising spherical liquid particles during deliquescence. We found that particles formed and grown in the chamber developed an asymmetric shape through coagulation. A transition to spherical shape was observed as the RH was increased to between 35% at  $-10^{\circ}\text{C}$  and 80% at  $-38^{\circ}\text{C}$ , confirming previous calculations of the viscosity transition conditions. Consequently,  $\alpha$ -pinene SOA particles exist in a viscous state over a wide range of ambient conditions, including the cirrus region of the free troposphere. This has implications for the physical, chemical and ice-nucleation properties of SOA and SOA-coated particles in the atmosphere.

## 1 Introduction

Organic particulate material is abundant in Earth's atmosphere. Biogenic and anthropogenic sources emit volatile organic compounds (VOCs), which are oxidised through a cascade of chemical reactions into extremely low volatility vapours that condense into the particle phase to form secondary organic aerosol (SOA) (Hallquist et al., 2009). Biogenic VOCs are much more abundant than anthropogenic VOCs (Guenther et al., 1995; Jimenez et al., 2009) and monoterpenes such as  $\alpha$ -pinene are found throughout the continental boundary layer, particularly in boreal forest regions (e.g., Tunved et al., 2006; Laaksonen et al., 2008). After formation, SOA influences climate on a global

### Observation of viscosity transition in $\alpha$ -pinene secondary organic aerosol

E. Järvinen et al.

Title Page

Abstract

Introduction

Conclusions

References

Tables

Figures



Back

Close

Full Screen / Esc

Printer-friendly Version

Interactive Discussion



scale directly by scattering and absorbing solar radiation and indirectly through aerosol-cloud interactions. Locally, SOA can affect air quality and human health (e.g., Nel, 2005; Huang et al., 2014). However, the chemical and physical processes that determine the properties of SOA particles are complex, and our understanding of these processes is limited (Hallquist et al., 2009; Hoyle et al., 2011).

Recently, considerable attention has been given to water uptake and viscous properties of SOA. It has been found that SOA particles can exist in the atmosphere in an amorphous semi-solid or solid state (Virtanen et al., 2010; Koop et al., 2011; Renbaum-Wolff et al., 2013; Pajunoja et al., 2014). The existence of these states has several atmospheric implications. Molecular diffusion in the condensed phase affects the gas uptake by viscous SOA particles and can, therefore, alter the SOA particle lifetime in the atmosphere (Shiraiwa et al., 2011). In addition, water uptake is inhibited in the viscous particles (Riipinen et al., 2012), limiting the SOA growth under conditions in which SOA would typically grow hygroscopically (Swietlicki et al., 2008; Pajunoja et al., 2015). This, in turn, influences the aerosol direct effect on radiative forcing. More recent studies have shown that the viscous SOA particles or their proxies can act as ice nuclei (IN) (Murray et al., 2010; Wagner et al., 2012; Wang et al., 2012; Wilson et al., 2012; Schill et al., 2014), thus influencing cloud cover, cloud optical properties, and precipitation.

In order to understand the climatological influence of the viscous state of SOA particles, detailed knowledge of the temperature and relative humidity (RH) ranges in which SOA can persist in a solid or semi-solid state is needed. Several experimental methods have been developed to measure the transition temperature or RH between different SOA phase states. A direct way to measure the glass transition temperature,  $T_g$ , of SOA substances is to use differential scanning calorimetry (DSC, Zobrist et al., 2008). However, this method requires the removal of the semivolatile aerosol particles from the surrounding gas, which can change the state, shape, or composition of the SOA particles. In contrast, indirect methods allow the sampling of the SOA particles with their surrounding gas. As indirect methods, they do not directly measure  $T_g$ , but rather probe the change in the SOA particle mechanical or aerodynamical properties with

## Observation of viscosity transition in $\alpha$ -pinene secondary organic aerosol

E. Järvinen et al.

Title Page

Abstract

Introduction

Conclusions

References

Tables

Figures



Back

Close

Full Screen / Esc

Printer-friendly Version

Interactive Discussion







## Observation of viscosity transition in $\alpha$ -pinene secondary organic aerosol

E. Järvinen et al.

Title Page

Abstract

Introduction

Conclusions

References

Tables

Figures

◀

▶

◀

▶

Back

Close

Full Screen / Esc

Printer-friendly Version

Interactive Discussion



linear or circular depolarisation in the exact backward direction, whereas non-spherical particles alter the depolarisation state of incident light depending on their size, shape, and refractive index. Therefore, depolarisation measurements can be used to determine the asphericity of isotropic particles. The magnitude of the depolarisation ratio can, in the case of aerosol particles, vary from only few per cent (in the case of sea salt) to up to 0.4 (in the case of dust aerosol) (Sakai et al., 2010). Solid or semi-solid amorphous particles may also induce depolarisation due to internal structures or inhomogeneous refractive index. In this case the depolarisation will depend on the gradient and/or variation of the refractive index as well as the size of the particle. In the case of sub-micron particles, the scale of the variation in particle properties is restricted by the size, and hence we can expect a maximum depolarisation ratio of 0.01 due to particle inhomogeneities, whereas the probable depolarisation ratios are well below that (Li et al., 2005; Dlugach and Mishchenko, 2015).

To quantify the extent of depolarisation, we define the the depolarisation ratio,  $\delta_{L,C}$  (indices L, C denoting the liner or circular incident depolarisation state) as the ratio of the intensity of the parallel polarised light,  $I_{\parallel}$ , to the perpendicular polarised light,  $I_{\perp}$ , in the backscatter direction when the particle is illuminated with perpendicularly polarised light. For a perfect measurement, we could take the ratio directly. In any real measurement there will be some background contribution to these two signals in the form of molecular scattering and scattering from chamber walls. Therefore, we subtract the background intensities  $I_{\parallel}^{bg}$  and  $I_{\perp}^{bg}$  measured in the absence of scattering particles from the measured scattered light intensities during particle measurements, defining  $\delta_{L,C}$  as

$$\delta_{L,C} = \frac{I_{\parallel} - I_{\parallel}^{bg}}{I_{\perp} - I_{\perp}^{bg}}. \quad (1)$$

We modelled the depolarisation ratio to assess the sensitivity of this method to the small particles that are produced in the environmental chamber and that will be used





to left-handed, although in this study we used only right-handed circular incident polarisation.

Two telescopes collect the laser light scattered from centre of the aerosol chamber at an angle of  $4^\circ$  in the forward direction and  $176^\circ$  in the backward direction. While the intensity in the forward scattering angle is directly measured with a photonmultiplier tube, the intensity in the backward scattering angle is decomposed into its polarisation components by a Wollaston prism. In the case of circular polarisation, the scattered light is first retarded to linear polarisation with a second liquid crystal variable retarder before the Wollaston prism.

### 3.2 Experimental setup

The experiments presented here were conducted at the CERN CLOUD chamber (Kirkby et al., 2011; Duplissy et al., 2015) during the CLOUD8 (November–December 2013) and CLOUD9 campaigns (September–November 2014). The chamber consists of a  $26\text{ m}^3$  stainless steel cylinder that is located inside a housing with thermal insulation. The temperature of the chamber can be varied from  $-60$  to  $100^\circ\text{C}$  and it is controlled by regulating the temperature of air flowing around the chamber and inside the thermal housing. During the CLOUD8 and CLOUD9 campaigns, the temperature inside the chamber was measured with a string of six thermocouples positioned horizontally at different distances between the wall and the chamber centre. We used the mean of the four inner thermocouples as a representative measure of the temperature in the chamber volume.

In the course of the experiments, air from the chamber was constantly sampled; and this sampled air was replaced with humidified artificial air to maintain a constant pressure inside the chamber. The artificial air was created by evaporating liquid nitrogen and oxygen, and humidified by passing part of the flow through a Nafion humidifier to achieve a chosen constant relative humidity (RH). Alternatively, the air was passed through a heated line to the chamber, allowing the dew point of the incoming air to be higher than that in the chamber. The heated line was used at temperatures of  $-30^\circ\text{C}$

## Observation of viscosity transition in $\alpha$ -pinene secondary organic aerosol

E. Järvinen et al.

Title Page

Abstract

Introduction

Conclusions

References

Tables

Figures



Back

Close

Full Screen / Esc

Printer-friendly Version

Interactive Discussion



## Observation of viscosity transition in $\alpha$ -pinene secondary organic aerosol

E. Järvinen et al.

Title Page

Abstract

Introduction

Conclusions

References

Tables

Figures



Back

Close

Full Screen / Esc

Printer-friendly Version

Interactive Discussion



or lower, to enable rapid RH increase. The water vapour was mixed with the main air stream before entering the chamber, which allowed a homogeneous RH throughout the chamber volume after a mixing time of few minutes (Voigtländer et al., 2012). The RH inside the chamber was measured with a chilled mirror dew point hygrometer (MBW, model 973). During CLOUD9 a tuneable diode laser (TDL system) was used to measure water vapour, in addition to the MBW. The newly installed tuneable diode laser system will be described in more detail in the following section.

SOA particles were produced within the CLOUD chamber by ozonolysis of gaseous  $\alpha$ -pinene; the two reactant gases were separately fed into the chamber through mass flow controllers. The ozone was monitored with a trace gas monitor ( $O_3$  analyser, Thermo Environmental Instruments, Inc., Model 49C);  $\alpha$ -pinene was measured by a PTR-TOF (Proton Transfer Reaction Time of Flight Mass Spectrometer, Ionicon Analytic). The ozone concentration was continuously measured, but, due to high concentrations of  $\alpha$ -pinene (over 600 ppbv), the PTR-TOF signal saturated, so it could not be measure continuously. The production of SOA was enhanced by UV photolysis of ozone to form OH radicals. A 50 W UV source (Philips TUV 130 W XPT lamp) was installed in a quartz tube inserted into the chamber. The formed OH oxidised  $\alpha$ -pinene to produce secondary organic vapours that nucleated and grew the aerosol particles.

Supporting measurements were provided by a range of instruments that were used to measure the physical and chemical composition of the aerosol particles inside the chamber. The chemical composition of the sub-micron aerosol particles was measured with an Aerodyne high-resolution time-of-flight aerosol mass spectrometer (HR-ToF AMS). From these measurements the atomic oxygen to carbon ratio (O / C) was determined. The size distribution of the aerosol particles was measured with an Ultra-High Sensitivity Aerosol Spectrometer (UHSAS, DMT), which measures the optical sphere equivalent diameter of the particles in a size range from approximately 60 to 1000 nm and with an SMPS, which measures the mobility diameter between 30 and 500 nm. The total concentration of aerosol particles was measured with a CPC (TSI 3010) with

a 10 nm cutoff and with a maximum detectable particle concentration of  $10\,000\text{ cm}^{-3}$  without coincidence corrections.

### 3.2.1 Relative humidity measurements

During the CLOUD9 campaign a tuneable diode laser (TDL) hygrometer, comparable to the APicT instrument as described by Fahey et al. (2014), was used to measure the water vapour content in-situ. The TDL has 1 Hz time resolution and employs a single optical path of 314 cm once across the mid-plane of the CERN CLOUD chamber. Its main component is a temperature-controlled, 10 mW distributed feedback diode laser (NTT Electronics) at a wavelength of  $(1370 \pm 1)\text{ nm}$ . The water absorption line was fitted on-line to determine water concentrations based on well-known spectroscopic constants. The windows mounted on the chamber limited the measurement range to between 30–1300 Pa water vapour pressure (300–13 000 ppm mixing ratio); the measurement uncertainty was  $\pm 7\%$  above 100 Pa and  $\pm 10\%$  between 30 and 100 Pa. The relative humidity in the CLOUD chamber was calculated using these humidity data together with the average temperatures measured with a horizontal string of four calibrated thermocouples at the mid-plane of the chamber. The two thermocouples near the wall were excluded due to wall temperature effect. The TDL hygrometer data enabled determination of the relative humidity even in the presence of clouds in the chamber, with an uncertainty of  $\pm 10\%$  above 100 Pa and  $\pm 13\%$  between 30 and 100 Pa water vapour pressure. The total humidity in the CLOUD chamber was also derived from the measurements from dew point hygrometer (model MBW973, MBW calibration Ltd.) attached to a heated sampling line.

### 3.2.2 Experimental procedure

The aim of the experiments was to determine if a slightly aspherical particle shape or internal inhomogeneity of the viscous amorphous SOA could be detected by sensitive, near-backscatter depolarisation measurements and, if so, to observe the transition

## Observation of viscosity transition in $\alpha$ -pinene secondary organic aerosol

E. Järvinen et al.

Title Page

Abstract

Introduction

Conclusions

References

Tables

Figures



Back

Close

Full Screen / Esc

Printer-friendly Version

Interactive Discussion



**Observation of  
viscosity transition in  
 $\alpha$ -pinene secondary  
organic aerosol**

E. Järvinen et al.

Title Page

Abstract

Introduction

Conclusions

References

Tables

Figures



Back

Close

Full Screen / Esc

Printer-friendly Version

Interactive Discussion



from irregular to a spherical shape during a phase transition as the RH was increased. The range of experiments required was determined using the T-matrix modelling together with the lowest detection limit of the SIMONE-Junior instrument as guidelines. Figure 2 demonstrates that, in order to measure a significant depolarisation signal with the highest aspect ratio (0.91), particles with a GMD of at least 600 nm must be generated. Furthermore, in contrast to atmospheric lidar applications (e.g., Sassen, 1991; Hirsikko et al., 2014), the detection volume of the SIMONE instrument is small, only a few cubic centimeters. This means that we would need a high concentration to have enough particles inside this small detection volume to produce measurable signals. We estimated that an initial concentration of  $10\,000\text{ cm}^{-3}$  newly formed SOA particles would produce adequate signals once the particles reached the size of 600 nm.

Each experiment commenced with clean, aerosol-free air (background concentration well below  $1\text{ cm}^{-3}$  and low RH (ranging from 5–15 %). The SOA particles were generated and grown in the chamber by continuous oxidation of  $\alpha$ -pinene (maximum concentration  $\sim 600$  ppbv) with ozone (maximum concentration  $\sim 700$  ppbv) to form low volatility oxidised organic compounds. SOA nucleation was initiated by injecting  $\alpha$ -pinene ( $10\text{ mL min}^{-1}$ ) and ozone ( $1000\text{ mL min}^{-1}$ ) into the chamber simultaneously for 1 to 7 min, depending on the chamber temperature, and then turning on the UV light. After 1 min the  $\alpha$ -pinene flow was turned off until the freshly nucleated particles had grown to a mean diameter of approximately 100 nm. This produced a near-monodisperse particle population. At this point the  $\alpha$ -pinene flow was turned back on and continuously injected into the chamber in order to grow the existing particles without inducing further new particle formation. The initial particle burst typically comprised around  $50\,000$ – $100\,000\text{ cm}^{-3}$   $\alpha$ -pinene SOA particles, which rapidly grew to about 20 nm diameter. After the particles had grown to diameters of approximately 600 nm, losses due to dilution, coagulation and the chamber walls had reduced the particle number concentration to  $5000$ – $10\,000\text{ cm}^{-3}$ . After a significant depolarisation signal had been detected, we increased the RH in the chamber to search for a transition to the liquid phase. The RH was gradually increased by injecting humidified air (RH 100 %) air into











tion signal. It should be possible to confirm this conclusion by simulating the scattering properties of the evolving spheroidal particles, but that is beyond the scope of this work and will be addressed in a future study.

As described in Sect. 3.1, secondary nucleation occurred in some of our experiments, resulting in a bimodal size distribution. Figure 9 shows such a run with two growing modes. The main mode was somewhat wider than in the single-mode experiments, so we do not see clear oscillations in the depolarisation signal. A new narrow mode was nucleated after 15:00 UTC, causing oscillations in the depolarisation signal, as the new mode grew. The measured depolarisation is, therefore, likely due to the net scattering and depolarisation contributions from both of these modes, making the interpretation of the depolarisation properties more challenging. Although the size distribution is not confined to a single size in the bimodal runs, the phase of the new particles was viscous, since the mode was formed before a significant increase in RH. The asphericity of the new mode is also observed in the oscillations that are caused by the newly nucleated narrow mode.

#### 4.4 The atomic oxygen to carbon ratio of the $\alpha$ -pinene SOA

The atomic oxygen to carbon (O / C) ratio of SOA particles increases with particle ageing and is related to the hygroscopicity of the particles (Massoli et al., 2010; Duplissy et al., 2011; Lambe et al., 2011). The O / C ratio affects the particle hardness; in the case of  $\alpha$ -pinene SOA particles, the hardness increases with increasing O / C ratio (Berkemeier et al., 2014). This might affect the particle shape and refractive index variation inside the particle, as higher hardness increases the possibility that the particles remain aspherical and thus induce higher depolarisation signal.

We measured the O / C ratio using the HR-ToF-AMS (Aiken et al., 2007, 2008). The measured O / C ratios varied from 0.23 to 0.29 with an average value of  $0.25 \pm 0.04$  (average  $\pm$  standard deviation). The O / C ratios decreased slightly with time during each experiment (Fig. 10). The average O / C ratio (below 0.3) is similar to that reported by Pajunoja et al. (2014) of laboratory produced  $\alpha$ -pinene SOA particles.

## Observation of viscosity transition in $\alpha$ -pinene secondary organic aerosol

E. Järvinen et al.

Title Page

Abstract

Introduction

Conclusions

References

Tables

Figures



Back

Close

Full Screen / Esc

Printer-friendly Version

Interactive Discussion



The SOA mass concentration shows a steep increase at the beginning of RUN2\_10C due to the continuous addition of ozone and alpha-pinene to the chamber. At 15:35 UTC the SOA production rate decreased slightly as the fresh supply of ozone was reduced. After switching off the ozone supply at 20:20 UTC the formation of SOA was stopped and as a result the SOA concentration decreased due to dilution.

#### 4.5 Measured viscosity-transition-RH as a function of temperature

The depolarisation signal in our experiments showed that the viscous  $\alpha$ -pinene SOA particles were non-spherical when the nucleation and growth of the particles occurred at low RH. As the RH increases, the highly viscous SOA particles start to take up water. The water uptake is slow, and proceeds gradually with increasing RH (Mikhailov et al., 2009; Zobrist et al., 2011). This is seen by the relatively slow shape transitions observed as the RH increases (Figs. 4 and 5). In the aqueous phase, the surface area is minimised to reach an energetically favourable state. The minimisation of the surface area results in shape change from aspherical to spherical. This change was observed in the depolarisation ratio at the end of the low-RH runs, as the depolarisation ratio decreased towards the instrument LOD. We determined the transition RH range from the measurements; the start of the transition was detected when the depolarisation ratio started to decrease significantly. The end of the transition was detected when the depolarisation ratio reached a constant level below the detection threshold (highlighted with grey in Figs. 4, 9, 8). The RH value at the time the depolarisation had decreased to a constant, zero level, describes the transition to an optically spherical shape. We label this RH value the viscosity-transition RH.

Figure 11 summarises the complete RH range, where the viscosity transition were observed for sub-zero temperatures. At 10 °C a depolarization signal over LOD was not observe, suggesting that the particles were already in a liquid state at 12 % RH. Generally, two results can be obtained from Fig. 11:

1. The viscosity-transition RH increases with decreasing temperature and

28594

## Observation of viscosity transition in $\alpha$ -pinene secondary organic aerosol

E. Järvinen et al.

Title Page

Abstract

Introduction

Conclusions

References

Tables

Figures



Back

Close

Full Screen / Esc

Printer-friendly Version

Interactive Discussion



2. the RH range, where the transition occurs becomes wider as the temperature decreases.

The viscosity-transition RH has near linear dependency of the temperature. At  $-10^{\circ}\text{C}$  the viscosity-transition occurred at RH around 35% and at  $-38^{\circ}\text{C}$  the transition was observed at around 80% RH. Result (ii) can be linked to the transition timescales, so that at colder temperatures the transition from a solid or semi-solid to liquid will last longer.

The viscosity-transition RH of the SOA particles does not directly provide the glass transition RH,  $\text{RH}_g$ , since the viscosity transition occurs near the full deliquescence relative humidity (FDRH), and the glass transition occurs when the relaxation timescales match the experimental timescale. The delay between the  $\text{RH}_g$  and the FDRH is governed by the competition between the humidification rate and timescale for water diffusion within the particle bulk (Berkemeier et al., 2014). We can expect that the viscosity transition is shifted to somewhat higher RH than the actual  $\text{RH}_g$  would be. Also it should be noted that the  $\text{RH}_g$  describes a change in the phase or state of a material at a constant composition, i.e., in a closed system. Our experiments probe the change as composition changes and this likely leads to a continuous variation in the  $\text{RH}_g$ . However, the advantage of our setup is that both the particle size and rate of change of RH, correspond roughly to those found in the atmosphere. Moreover, the transition timescales that we observed, 10 s of minutes, are relevant to those that we can expect in the atmosphere. Consequently, the viscosity transition RH that we report is relevant for the atmospheric processes and, therefore, can be compared to  $\text{RH}_g$  in an atmospheric context.

We compared our results with the Koop et al. (2011) generic SOA estimate that predicts the glass transition temperature as a function of RH for a broad variety of SOA (Fig. 11). Overall the results agree well with the generic SOA estimate, and significantly reduce the uncertainty in that estimate. Moreover, our results suggest the relationship between the transition RH and the temperature is more linear than predicted by Koop et al. (2011). This may be especially relevant at high RH, where we can expect that the

Observation of  
viscosity transition in  
 $\alpha$ -pinene secondary  
organic aerosol

E. Järvinen et al.

Title Page

Abstract

Introduction

Conclusions

References

Tables

Figures



Back

Close

Full Screen / Esc

Printer-friendly Version

Interactive Discussion





above the homogeneous freezing threshold, but, to better understand the phase state of SOA in the cirrus regime, future studies at lower temperatures are needed.

## 5 Conclusions

The influence of temperature and relative humidity on the viscosity transition of SOA particles is a subject of considerable uncertainty (Koop et al., 2011). Here, we measured the viscosity transition RH at different atmospherically-relevant temperatures using a new optical and non-invasive in-situ method. We used near-backscattering depolarisation to measure the asphericity of the SOA particles and the shape change to spherical at near the full deliquescence relative humidity. The relaxation timescales were observed to be 10 s of minutes – time scales relevant for atmospheric processes. Thus, we conclude that the viscosity transition RH provides a quantity that is directly relevant for glassy transitions of SOA particles in the atmosphere.

We showed that  $\alpha$ -pinene SOA particles acquire a non-spherical shape due to coagulation in our chamber experiments. The non-spherical shape persists when the particles are nucleated and grown under low RH. This non-spherical shape is a result of the viscosity of the particles and this viscous state can be detected with depolarisation measurements for SOA particles larger than 100 nm.

We observed the viscosity transition in six experiments conducted at at four temperatures. We found that the viscosity transition temperature depends linearly on RH. This increases the likelihood that  $\alpha$ -pinene SOA particles persist in a viscous state at low temperatures, making them potential ice nuclei (IN) in the cirrus cloud regime. Generally, our results improve the understanding of the viscosity transition temperature RH at temperatures above the homogeneous freezing point. The influence of highly viscous SOA on climate should be further assessed in future modelling studies.

*Acknowledgements.* We would like to thank CERN for supporting CLOUD with important technical and financial resources. We thank the CLOUD-TRAIN community and specially all the ITN-students for their help and support. This research has received funding from the Sev-

28597

ACPD

15, 28575–28617, 2015

## Observation of viscosity transition in $\alpha$ -pinene secondary organic aerosol

E. Järvinen et al.

Title Page

Abstract

Introduction

Conclusions

References

Tables

Figures

◀

▶

◀

▶

Back

Close

Full Screen / Esc

Printer-friendly Version

Interactive Discussion



enth Framework Programme of the European Union (Marie Curie-Networks for Initial Training MC-ITN CLOUD-TRAIN no. 316662), from Swiss National Science Foundation (SNSF) grant number 200021\_140663, from US National Science Foundation Grants AGS-1447056 and AGS-1439551, from Dreyfus Award EP-11-117, from German Federal Ministry of Education and Research BMBF (project no. 01LK1222A and B), from the Davidow Foundation, and from the funding of the German Federal Ministry of Education and Research (BMBF) through the CLOUD12 project.

The article processing charges for this open-access publication were covered by a Research Centre of the Helmholtz Association.

## References

- Adler, G., Koop, T., Haspel, C., Taraniuk, I., Moise, T., Koren, I., Heiblum, R. H., and Rudich, Y.: Formation of highly porous aerosol particles by atmospheric freeze-drying in ice clouds, *P. Natl. Acad. Sci. USA*, 110, 20414–20419, doi:10.1073/pnas.1317209110, 2013. 28579
- Aiken, A. C., DeCarlo, P. F., and Jimenez, J. L.: Elemental analysis of organic species with electron ionization high-resolution mass spectrometry, *Anal. Chem.*, 79, 8350–8358, 2007. 28593
- Aiken, A. C., Decarlo, P. F., Kroll, J. H., Worsnop, D. R., Huffman, J. A., Docherty, K. S., Ulbrich, I. M., Mohr, C., Kimmel, J. R., Sueper, D., Sun, Y., Zhang, Q., Trimborn, A., Northway, M., Ziemann, P. J., Canagaratna, M. R., Onasch, T. B., Alfarra, M. R., Prevot, A. S. H., Dommen, J., Duplissy, J., Metzger, A., Baltensperger, U., and Jimenez, J. L.: O/C and OM/OC ratios of primary, secondary, and ambient organic aerosols with high-resolution time-of-flight aerosol mass spectrometry, *Environ. Sci. Technol.*, 42, 4478–4485, 2008. 28593
- Bateman, A. P., Belassein, H., and Martin, S. T.: Impactor apparatus for the study of particle rebound: Relative humidity and capillary forces, *Aerosol Sci. Tech.*, 48, 42–52, 2014. 28579
- Berkemeier, T., Shiraiwa, M., Pöschl, U., and Koop, T.: Competition between water uptake and ice nucleation by glassy organic aerosol particles, *Atmos. Chem. Phys.*, 14, 12513–12531, doi:10.5194/acp-14-12513-2014, 2014. 28593, 28595

## Observation of viscosity transition in $\alpha$ -pinene secondary organic aerosol

E. Järvinen et al.

Title Page

Abstract

Introduction

Conclusions

References

Tables

Figures



Back

Close

Full Screen / Esc

Printer-friendly Version

Interactive Discussion







**Observation of  
viscosity transition in  
 $\alpha$ -pinene secondary  
organic aerosol**

E. Järvinen et al.

Title Page

Abstract

Introduction

Conclusions

References

Tables

Figures



Back

Close

Full Screen / Esc

Printer-friendly Version

Interactive Discussion

Schneider, J., Drewnick, F., Borrmann, S., Weimer, S., Demerjian, K., Salcedo, D., Cottrell, L., Griffin, R., Takami, A., Miyoshi, T., Hatakeyama, S., Shimono, A., Sun, J. Y., Zhang, Y. M., Dzepina, K., Kimmel, J. R., Sueper, D., Jayne, J. T., Herndon, S. C., Trimborn, A. M., Williams, L. R., Wood, E. C., Middlebrook, A. M., Kolb, C. E., Baltensperger, U., and Worsnop, D. R.: Evolution of organic aerosols in the atmosphere, *Science*, 326, 1525–1529, 2009. 28577

Kirkby, J., Curtius, J., Almeida, J., Dunne, E., Duplissy, J., Ehrhart, S., Franchin, A., Gagné, S., Ickes, L., Kürten, A., et al.: Role of sulphuric acid, ammonia and galactic cosmic rays in atmospheric aerosol nucleation, *Nature*, 476, 429–433, 2011. 28584, 28591

Koop, T., Bookhold, J., Shiraiwa, M., and Pöschl, U.: Glass transition and phase state of organic compounds: dependency on molecular properties and implications for secondary organic aerosols in the atmosphere, *Phys. Chem. Chem. Phys.*, 13, 19238–19255, 2011. 28578, 28595, 28596, 28597, 28617

Kulmala, M., Riipinen, I., Sipilä, M., Manninen, H. E., Petäjä, T., Junninen, H., Dal Maso, M., Mordas, G., Mirme, A., Vana, M., Hirsikko, A., Laakso, L., Harrison, R. M., Hanson, I., Leung, C., Lehtinen, K. E. J., and Kerminen, V. M.: Toward direct measurement of atmospheric nucleation, *Science*, 318, 89–92, 2007. 28591

Kulmala, M., Kontkanen, J., Junninen, H., Lehtipalo, K., Manninen, H. E., Nieminen, T., Petäjä, T., Sipilä, M., Schobesberger, S., Rantala, P., Franchin, A., Jokinen, T., Järvinen, E., Äijälä, M., Kangasluoma, J., Hakala, J., Aalto, P. P., Paasonen, P., Mikkilä, J., Vanhanen, J., Aalto, J., Hakola, H., Makkonen, U., Ruuskanen, T., Mauldin III, R. L., Duplissy, J., Vehkamäki, H., Bäck, J., Kortelainen, A., Riipinen, I., Kurtén, T., Johnston, M. V., Smith, J. N., Ehn, M., Mentel, T. F., Lehtinen, K. E. J., Laaksonen, A., Kerminen, V. M., and Worsnop, D. R.: Direct observations of atmospheric aerosol nucleation, *Science*, 339, 943–946, 2013. 28591

Laaksonen, A., Kulmala, M., O'Dowd, C. D., Joutsensaari, J., Vaattovaara, P., Mikkonen, S., Lehtinen, K. E. J., Sogacheva, L., Dal Maso, M., Aalto, P., Petäjä, T., Sogachev, A., Yoon, Y. J., Lihavainen, H., Nilsson, D., Facchini, M. C., Cavalli, F., Fuzzi, S., Hoffmann, T., Arnold, F., Hanke, M., Sellegri, K., Umann, B., Junkermann, W., Coe, H., Allan, J. D., Alfarra, M. R., Worsnop, D. R., Riekkola, M. -L., Hyötyläinen, T., and Viisanen, Y.: The role of VOC oxidation products in continental new particle formation, *Atmos. Chem. Phys.*, 8, 2657–2665, doi:10.5194/acp-8-2657-2008, 2008. 28577

**Observation of  
viscosity transition in  
 $\alpha$ -pinene secondary  
organic aerosol**

E. Järvinen et al.

Title Page

Abstract

Introduction

Conclusions

References

Tables

Figures



Back

Close

Full Screen / Esc

Printer-friendly Version

Interactive Discussion



- Lambe, A. T., Onasch, T. B., Massoli, P., Croasdale, D. R., Wright, J. P., Ahern, A. T., Williams, L. R., Worsnop, D. R., Brune, W. H., and Davidovits, P.: Laboratory studies of the chemical composition and cloud condensation nuclei (CCN) activity of secondary organic aerosol (SOA) and oxidized primary organic aerosol (OPOA), *Atmos. Chem. Phys.*, 11, 8913–8928, doi:10.5194/acp-11-8913-2011, 2011. 28593
- Li, X., Taflove, A., and Backman, V.: Quantitative analysis of depolarization of backscattered light by stochastically inhomogeneous dielectric particles, *Opt. Lett.*, 30, 902–904, 2005. 28581
- Massoli, P., Lambe, A., Ahern, A., Williams, L., Ehn, M., Mikkilä, J., Canagaratna, M., Brune, W., Onasch, T., Jayne, J., Petäjä, T., Kulmala, M., Laaksonen, A., Kolb, C. E., Davidovits, P., and Worsnop, D. R.: Relationship between aerosol oxidation level and hygroscopic properties of laboratory generated secondary organic aerosol (SOA) particles, *Geophys. Res. Lett.*, 37, L24801, doi:10.1029/2010GL045258, 2010. 28593
- Mikhailov, E., Vlasenko, S., Martin, S. T., Koop, T., and Pöschl, U.: Amorphous and crystalline aerosol particles interacting with water vapor: conceptual framework and experimental evidence for restructuring, phase transitions and kinetic limitations, *Atmos. Chem. Phys.*, 9, 9491–9522, doi:10.5194/acp-9-9491-2009, 2009. 28594
- Mishchenko, M. and Hovenier, J.: Depolarization of light backscattered by randomly oriented nonspherical particles, *Opt. Lett.*, 20, 1356–1358, 1995. 28592
- Mishchenko, M., Travis, L., and Mackowski, D.: T-matrix computations of light scattering by nonspherical particles: a review, *J. Quant. Spectrosc. Ra.*, 55, 535–575, 1996. 28582
- Murray, B. J., Wilson, T. W., Dobbie, S., Cui, Z., Al-Jumur, S. M., Möhler, O., Schnaiter, M., Wagner, R., Benz, S., Niemand, M., Saathoff, H., Ebert, V., Wagner, S., and Kärcher, B.: Heterogeneous nucleation of ice particles on glassy aerosols under cirrus conditions, *Nat. Geosci.*, 3, 233–237, 2010. 28578
- Naumann, K.-H.: COSIMA – a computer program simulating the dynamics of fractal aerosols, *J. Aerosol Sci.*, 34, 1371–1397, 2003. 28590
- Nel, A.: Air pollution-related illness: effects of particles, *Science*, 308, 804–806, doi:10.1126/science.1108752, 2005. 28578
- Pajunoja, A., Malila, J., Hao, L., Joutsensaari, J., Lehtinen, K. E., and Virtanen, A.: Estimating the viscosity range of SOA particles based on their coalescence time, *Aerosol Sci. Tech.*, 48, i–iv, 2014. 28578, 28579, 28593



**Observation of  
viscosity transition in  
 $\alpha$ -pinene secondary  
organic aerosol**

E. Järvinen et al.

Title Page

Abstract

Introduction

Conclusions

References

Tables

Figures



Back

Close

Full Screen / Esc

Printer-friendly Version

Interactive Discussion



– cloud chamber measurements in the context of contrail and cirrus microphysics, *Atmos. Chem. Phys.*, 12, 10465–10484, doi:10.5194/acp-12-10465-2012, 2012. 28582, 28583, 28588

5 Schnitzhofer, R., Metzger, A., Breitenlechner, M., Jud, W., Heinritzi, M., De Menezes, L.-P., Duplissy, J., Guida, R., Haider, S., Kirkby, J., Mathot, S., Minginette, P., Onnela, A., Walther, H., Wasem, A., Hansel, A., and the CLOUD Team: Characterisation of organic contaminants in the CLOUD chamber at CERN, *Atmos. Meas. Tech.*, 7, 2159–2168, doi:10.5194/amt-7-2159-2014, 2014. 28580

10 Shiraiwa, M., Ammann, M., Koop, T., and Pöschl, U.: Gas uptake and chemical aging of semisolid organic aerosol particles, *P. Natl. Acad. Sci. USA*, 108, 11003–11008, 2011. 28578

15 Swietlicki, E., HANSSON, H.-C., Hämeri, K., Svenningsson, B., Massling, A., McFiggans, G., McMurry, P., Petäjä, T., Tunved, P., Gysel, M., Topping, D. Weingartner, E., Baltensperger, U., Rissler, J., Wiedensohler, A., and Kulmala, M.: Hygroscopic properties of submicrometer atmospheric aerosol particles measured with H-TDMA instruments in various environments – a review, *Tellus B*, 60, 432–469, 2008. 28578

Tunved, P., Hansson, H.-C., Kerminen, V.-M., Ström, J., Dal Maso, M., Lihavainen, H., Viisanen, Y., Aalto, P., Komppula, M., and Kulmala, M.: High natural aerosol loading over boreal forests, *Science*, 312, 261–263, 2006. 28577

20 Virtanen, A., Joutsensaari, J., Koop, T., Kannosto, J., Yli-Pirilä, P., Leskinen, J., Mäkelä, J. M., Holopainen, J. K., Pöschl, U., Kulmala, M., Worsnop, D. R., and Laaksonen, A.: An amorphous solid state of biogenic secondary organic aerosol particles, *Nature*, 467, 824–827, 2010. 28578, 28579, 28591

25 Virtanen, A., Kannosto, J., Kuuluvainen, H., Arffman, A., Joutsensaari, J., Saukko, E., Hao, L., Yli-Pirilä, P., Tiitta, P., Holopainen, J. K., Keskinen, J., Worsnop, D. R., Smith, J. N., and Laaksonen, A.: Bounce behavior of freshly nucleated biogenic secondary organic aerosol particles, *Atmos. Chem. Phys.*, 11, 8759–8766, doi:10.5194/acp-11-8759-2011, 2011. 28590

Voigtländer, J., Duplissy, J., Rondo, L., Kürten, A., and Stratmann, F.: Numerical simulations of mixing conditions and aerosol dynamics in the CERN CLOUD chamber, *Atmos. Chem. Phys.*, 12, 2205–2214, doi:10.5194/acp-12-2205-2012, 2012. 28585

30 Wagner, R., Möhler, O., Saathoff, H., Schnaiter, M., Skrotzki, J., Leisner, T., Wilson, T. W., Malkin, T. L., and Murray, B. J.: Ice cloud processing of ultra-viscous/glassy aerosol particles leads to enhanced ice nucleation ability, *Atmos. Chem. Phys.*, 12, 8589–8610, doi:10.5194/acp-12-8589-2012, 2012. 28578

**Observation of  
viscosity transition in  
 $\alpha$ -pinene secondary  
organic aerosol**

E. Järvinen et al.

Title Page

Abstract

Introduction

Conclusions

References

Tables

Figures

◀

▶

◀

▶

Back

Close

Full Screen / Esc

Printer-friendly Version

Interactive Discussion



- Wang, B., Lambe, A. T., Massoli, P., Onasch, T. B., Davidovits, P., Worsnop, D. R., and Knopf, D. A.: The deposition ice nucleation and immersion freezing potential of amorphous secondary organic aerosol: pathways for ice and mixed-phase cloud formation, *J. Geophys. Res.-Atmos.*, 117, D16209, doi:10.1029/2012JD018063, 2012. 28578
- 5 Wilson, T. W., Murray, B. J., Wagner, R., Möhler, O., Saathoff, H., Schnaiter, M., Skrotzki, J., Price, H. C., Malkin, T. L., Dobbie, S., and Al-Jumur, S. M. R. K.: Glassy aerosols with a range of compositions nucleate ice heterogeneously at cirrus temperatures, *Atmos. Chem. Phys.*, 12, 8611–8632, doi:10.5194/acp-12-8611-2012, 2012. 28578
- 10 Zhang, Y., Sanchez, M. S., Douet, C., Wang, Y., Bateman, A. P., Gong, Z., Kuwata, M., Renbaum-Wolff, L., Sato, B. B., Liu, P. F., Bertram, A. K., Geiger, F. M., and Martin, S. T.: Changing shapes and implied viscosities of suspended submicron particles, *Atmos. Chem. Phys. Discuss.*, 15, 6821–6850, doi:10.5194/acpd-15-6821-2015, 2015. 28579
- Zobrist, B., Marcolli, C., Pedernera, D. A., and Koop, T.: Do atmospheric aerosols form glasses?, *Atmos. Chem. Phys.*, 8, 5221–5244, doi:10.5194/acp-8-5221-2008, 2008. 28578
- 15 Zobrist, B., Soonsin, V., Luo, B. P., Krieger, U. K., Marcolli, C., Peter, T., and Koop, T.: Ultra-slow water diffusion in aqueous sucrose glasses, *Phys. Chem. Chem. Phys.*, 13, 3514–3526, 2011. 28594

## Observation of viscosity transition in $\alpha$ -pinene secondary organic aerosol

E. Järvinen et al.

**Table 1.** Experiment list with experiment run number, starting temperature, relative humidity at the beginning, particle size before transition started and measured relative humidity range for the viscosity transition.

| Run       | CLOUD run number | $T$ [°C] | Start RH [%]    | Transition mode mean diameter [nm] | Viscosity transition RH [%] |
|-----------|------------------|----------|-----------------|------------------------------------|-----------------------------|
| RUN_10C   | CLOUD8 1313      | 10       | 12              | no transition                      | no transition               |
| RUN1_-10C | CLOUD8 1314      | -10      | 12              | 560                                | 23–35                       |
| RUN2_-10C | CLOUD9 1511      | -10      | 12              | 880                                | 31–36                       |
| RUN1_-20C | CLOUD9 1512      | -20      | 10              | 500, 850 <sup>2</sup>              | 44–49                       |
| REF_-20C  | CLOUD9 1513      | -20      | 60 <sup>1</sup> | no transition                      | no transition               |
| RUN2_-20C | CLOUD9 1514      | -20      | 4               | 1000                               | 41–45                       |
| RUN_-30C  | CLOUD9 1515      | -30      | 2               | 500, 850 <sup>2</sup>              | 55–62                       |
| RUN_-38C  | CLOUD9 1516      | -38      | 5               | 630                                | 69–79                       |

<sup>1</sup> RH varied between 60 and 70 %.

<sup>2</sup> More than one mode present.

Title Page

Abstract

Introduction

Conclusions

References

Tables

Figures

◀

▶

◀

▶

Back

Close

Full Screen / Esc

Printer-friendly Version

Interactive Discussion



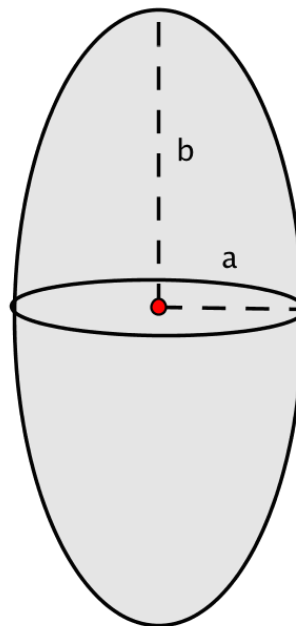
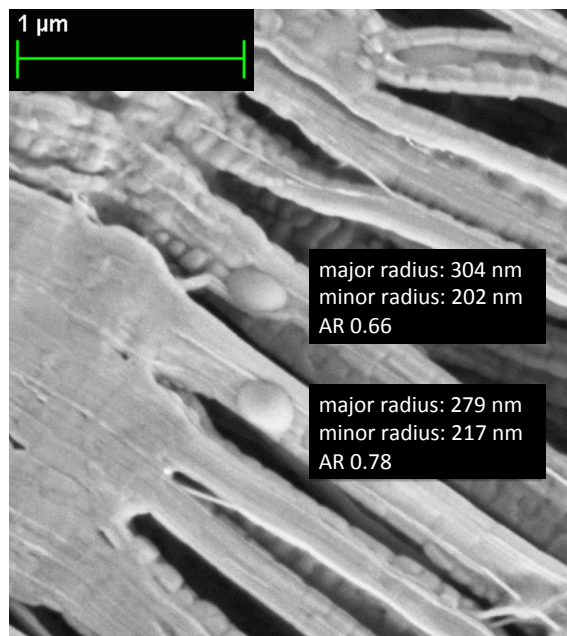


**Figure 1.** The SOA particles were modelled as prolate spheroids. An ESEM image of the SOA particles sampled from the CLOUD chamber show a spheroidal “egg-like” shape. The shape of the SOA particles in the ESEM images does not necessary resemble the real shape of the particles in the chamber, due to sampling conditions. In the T-matrix notation the aspect ratio (AR) is determined as the relation between the equatorial radius to the polar radius ( $a/b$ ) and is thus  $< 1$  for prolate spheroids.

Observation of viscosity transition in  $\alpha$ -pinene secondary organic aerosol

E. Järvinen et al.

Title Page

Abstract Introduction

Conclusions References

Tables Figures

◀ ▶

◀ ▶

Back Close

Full Screen / Esc

Printer-friendly Version

Interactive Discussion



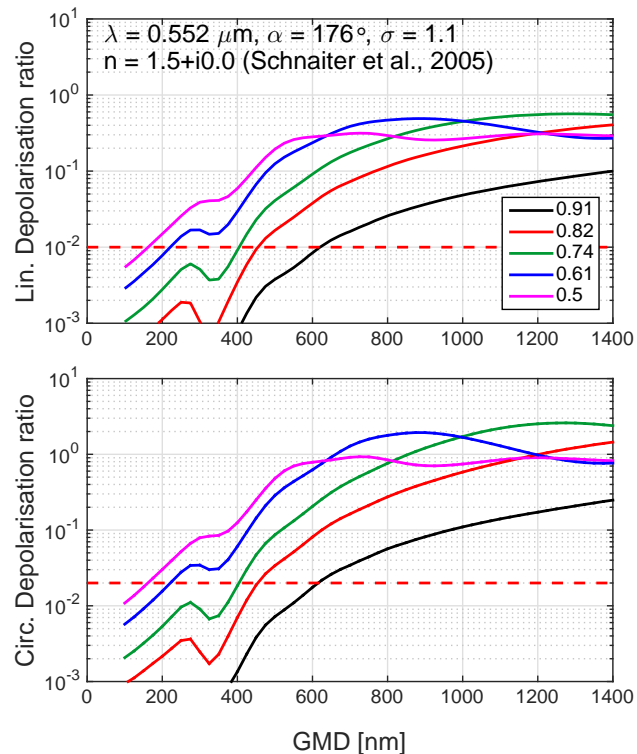


**Figure 2.** To plan the experiment, the expected linear and circular depolarisation ratios were modelled with the T-matrix model assuming a spheroidal shape. A narrow particle size distribution with a constant GSD of 1.1 was used in the model and the GMD of the particles was varied from 0 to 1400 nm ( $x$  axis). The calculation was made for five spheroidal shapes with aspect ratios ranging from 0.91 to 0.5. The detection thresholds of the SIMONE-Junior instrument (1 % for linear depolarisation and 2 % for circular) are indicated as dashed red horizontal lines. The modelling study indicates that the SOA particles need to be grown past 600 nm to produce a detectable depolarisation ratio at aspect ratios up to 0.91.

**Observation of  
viscosity transition in  
 $\alpha$ -pinene secondary  
organic aerosol**

E. Järvinen et al.

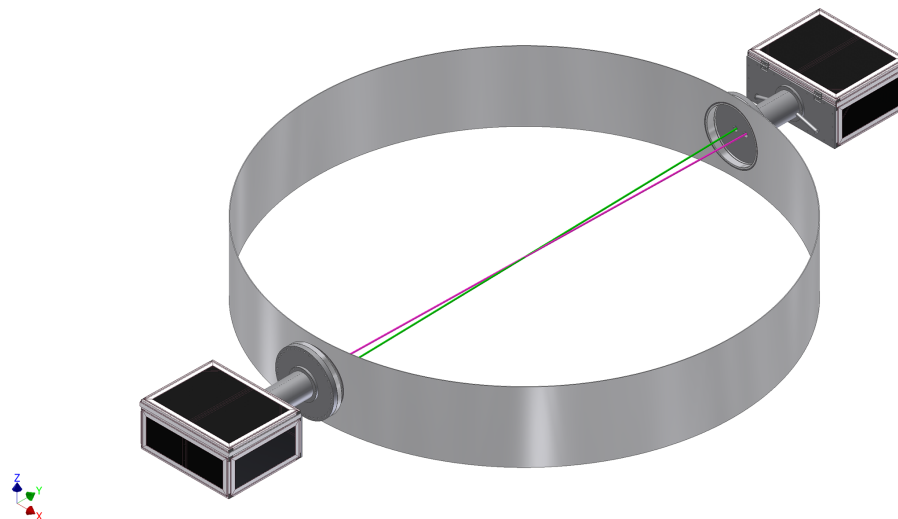


**Figure 3.** The SIMONE setup at the CERN CLOUD chamber. The instrument consists of two boxes facing each other. One box houses the laser production and the backward scattered light detector and the other box houses the forward scattered light detector and a beam dump. The green line illustrates the path of the laser beam, which crosses the field of view (purple line) of the detection optics. The overlap region defines a detection volume of a few cubic centimetres volume in the centre of the chamber.

[Title Page](#)[Abstract](#)[Introduction](#)[Conclusions](#)[References](#)[Tables](#)[Figures](#)[◀](#)[▶](#)[◀](#)[▶](#)[Back](#)[Close](#)[Full Screen / Esc](#)[Printer-friendly Version](#)[Interactive Discussion](#)

## Observation of viscosity transition in $\alpha$ -pinene secondary organic aerosol

E. Järvinen et al.

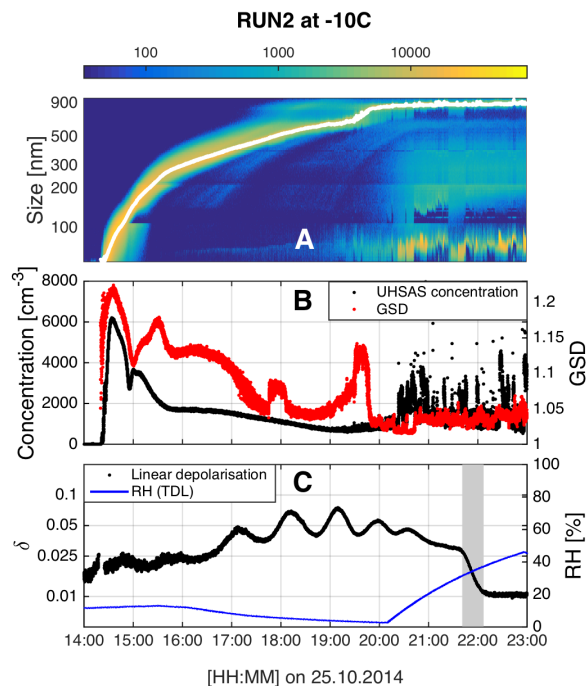


**Figure 4.** Overview of RUN2 at  $-10^{\circ}\text{C}$ . The particle size distribution and the GMD from a log-normal fit are shown in panel (a). Panel (b) shows the total concentration measured with the UHSAS (with 56 nm cutoff) and the GSD determined from a log-normal fit. Panel (c) shows the linear depolarisation ratio and RH. The RH was kept low during the growth of the SOA particles, allowing them to remain in a viscous state. The RH was raised after about 20:15 UTC in order to measure its value at the particle phase transition from highly viscous to low viscosity state. The gradual phase transition began at 21:41 UTC and is indicated by the grey area in panel (c). The top and middle panels show further particle nucleation starting around 19:00 UTC; these particles remained relatively small and did not affect the measurement.

## Observation of viscosity transition in $\alpha$ -pinene secondary organic aerosol

E. Järvinen et al.

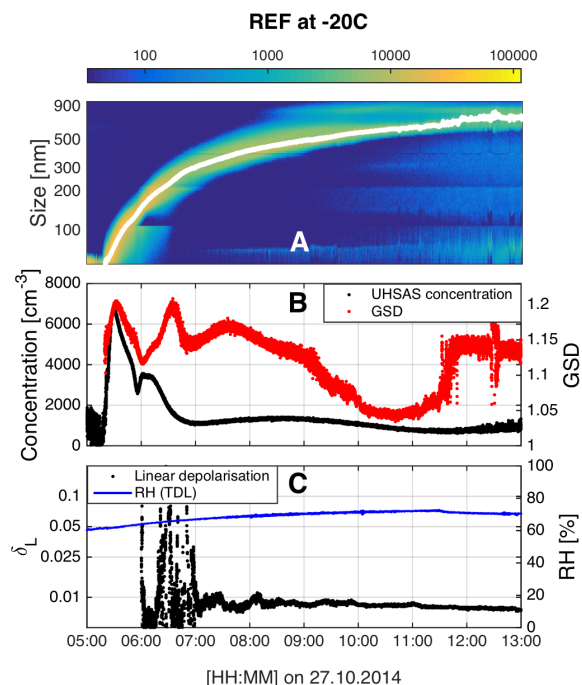


**Figure 5.** Overview of the reference run at  $-20^{\circ}\text{C}$ . As for Fig. 4, panel (a) shows the particle size distribution and the GMD from a log-normal fit. Panel (b) shows the total concentration measured with the UHSAS (with 56 nm cutoff) and the GSD determined from a log-normal fit. Panel (c) shows the time-development of the linear depolarisation ratio and the RH. During the reference run the RH was kept over 60 % during the growth of the SOA particles to ensure that they remained in low viscous state during growth. The linear depolarisation ratio stayed below the detection threshold during the entire experiment, indicating a low viscous state of the particles and verifying the absence of measurement artifacts.

Observation of  
viscosity transition in  
 $\alpha$ -pinene secondary  
organic aerosol

E. Järvinen et al.

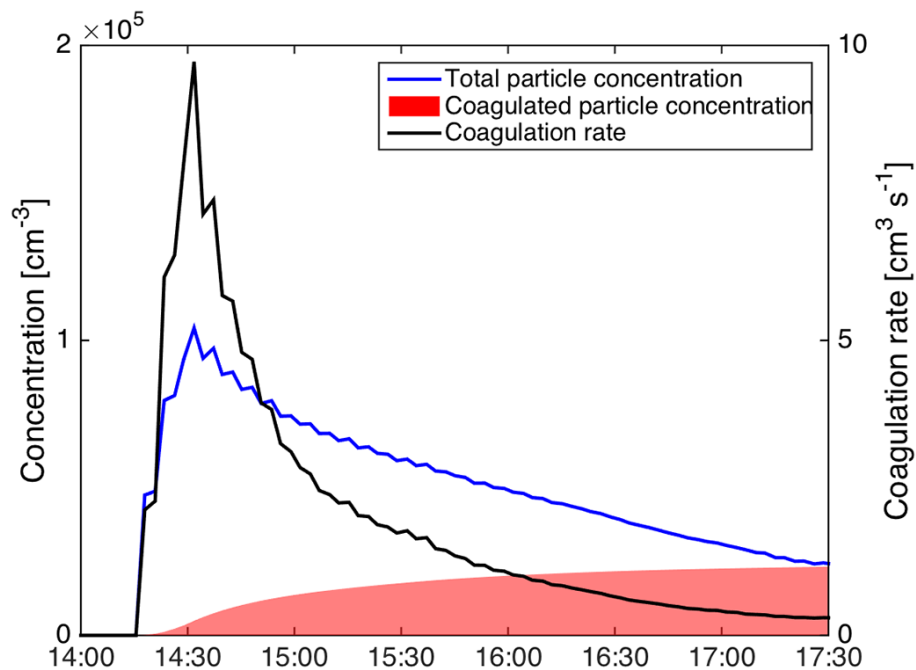


**Figure 6.** COSIMA model results for the coagulation rate of the SOA particles during experiment RUN2 at  $-10^\circ\text{C}$ . The particle number concentration was integrated from the SMPS measurements between 20 and 500 nm.

[Title Page](#)[Abstract](#)[Introduction](#)[Conclusions](#)[References](#)[Tables](#)[Figures](#)[◀](#)[▶](#)[◀](#)[▶](#)[Back](#)[Close](#)[Full Screen / Esc](#)[Printer-friendly Version](#)[Interactive Discussion](#)

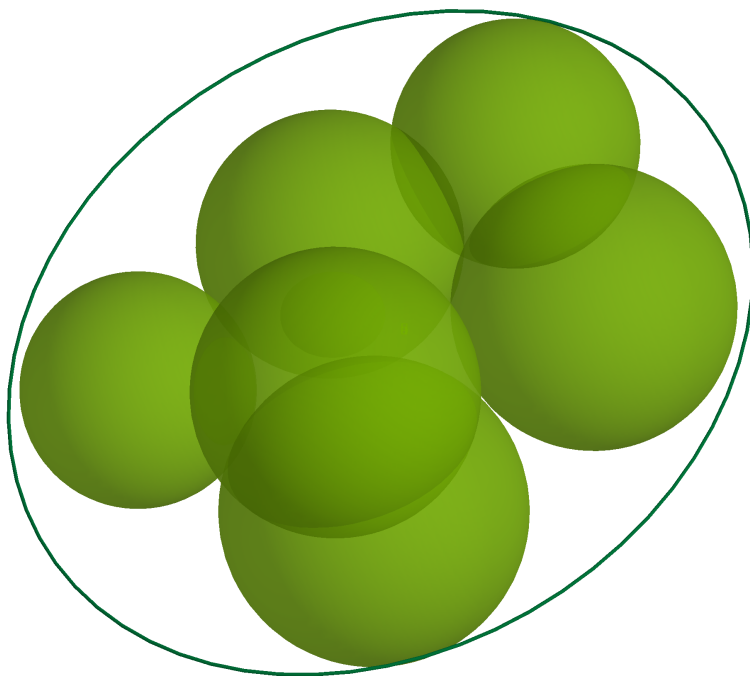


**Figure 7.** The SOA particles form aggregates at the early stage of their growth. After the coagulation rate has slowed, the aggregates grow by vapour condensation to form non-spherical particles. The number of the single SOA particles in the aggregate is illustrative and does not necessary describe the real aggregates in the CLOUD chamber.

Observation of viscosity transition in  $\alpha$ -pinene secondary organic aerosol

E. Järvinen et al.

Title Page

Abstract

Introduction

Conclusions

References

Tables

Figures

◀

▶

◀

▶

Back

Close

Full Screen / Esc

Printer-friendly Version

Interactive Discussion



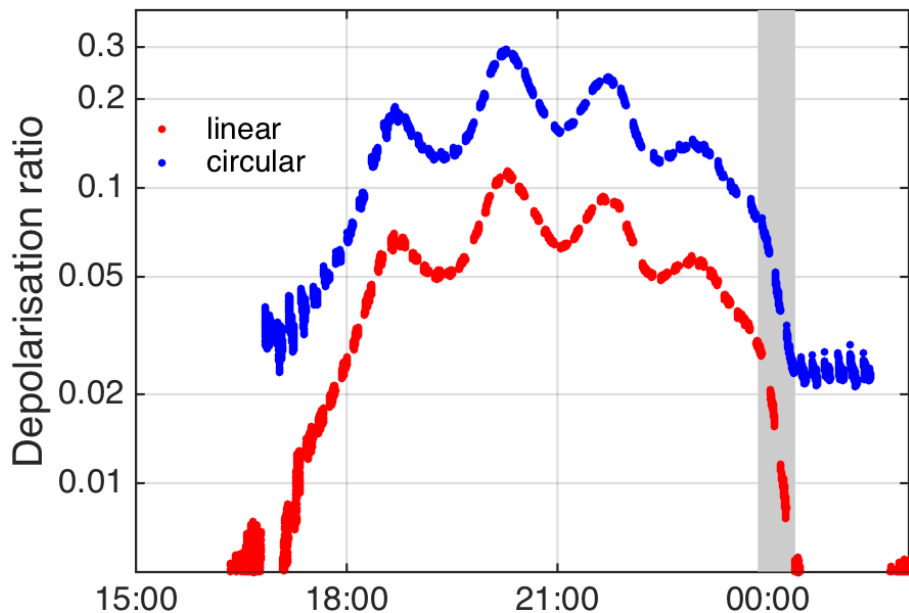


**Figure 8.** An example of alternating measurements of the linear and the circular depolarisation ratios during RUN\_-30C. Both depolarisation ratios show oscillations with consistent minima and maxima. The shape transition is indicated by the grey area.

Observation of viscosity transition in  $\alpha$ -pinene secondary organic aerosol

E. Järvinen et al.

Title Page

Abstract

Introduction

Conclusions

References

Tables

Figures

◀

▶

◀

▶

Back

Close

Full Screen / Esc

Printer-friendly Version

Interactive Discussion



## Observation of viscosity transition in $\alpha$ -pinene secondary organic aerosol

E. Järvinen et al.

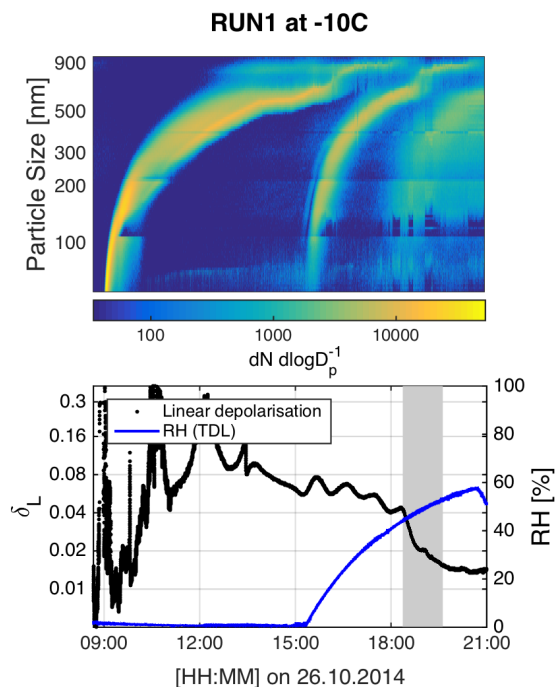


**Figure 9.** An example of a run with two growing SOA particle modes. The primary mode nucleated around 09:00 UTC and reached a median size of 600 nm around 15:00 UTC, when a second nucleation burst occurred. The new narrow mode produced the oscillations seen in the depolarisation ratio after 15:00 UTC. The main mode was too wide and did not cause oscillations. These particles exhibited a phase transition starting around 18:25 UTC. The noise in the depolarisation signal at the start of the experiment is caused by low signal in the backward detectors.

Observation of  
viscosity transition in  
 $\alpha$ -pinene secondary  
organic aerosol

E. Järvinen et al.

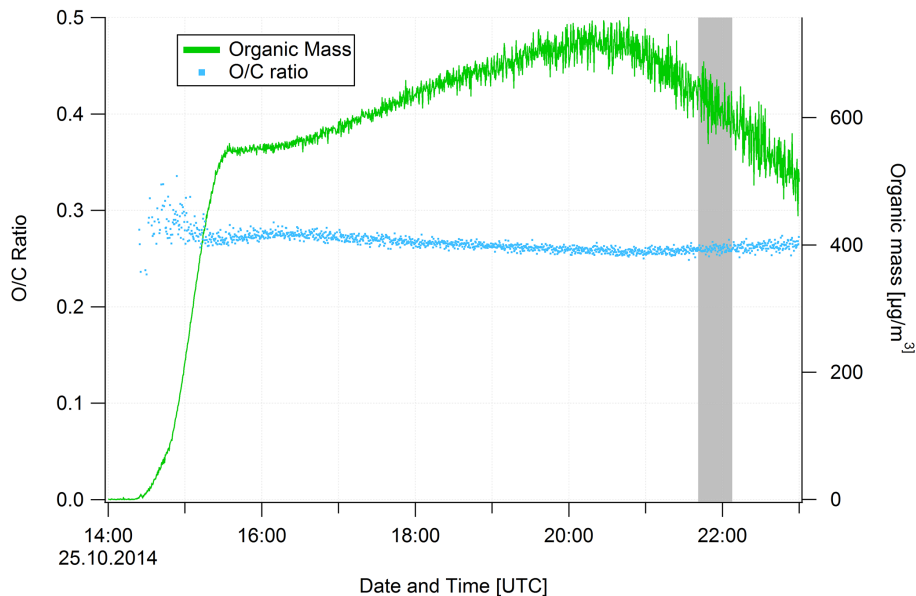


**Figure 10.** SOA mass concentration (green trace) and O/C ratio of the SOA particles (blue points) measured with the HR-ToF AMS for RUN1\_-10C. The grey highlighted area represents the phase transition. The mass concentration represents SOA formed via  $\alpha$ -pinene ozonolysis; ozone was first added to the chamber during the period of steep growth at the beginning of the experiment. The decrease in SOA concentration towards the end of the experiment was due to dilution. The O/C ratio stayed almost constant throughout the experiment.

[Title Page](#)[Abstract](#)[Introduction](#)[Conclusions](#)[References](#)[Tables](#)[Figures](#)[◀](#)[▶](#)[◀](#)[▶](#)[Back](#)[Close](#)[Full Screen / Esc](#)[Printer-friendly Version](#)[Interactive Discussion](#)

## Observation of viscosity transition in $\alpha$ -pinene secondary organic aerosol

E. Järvinen et al.

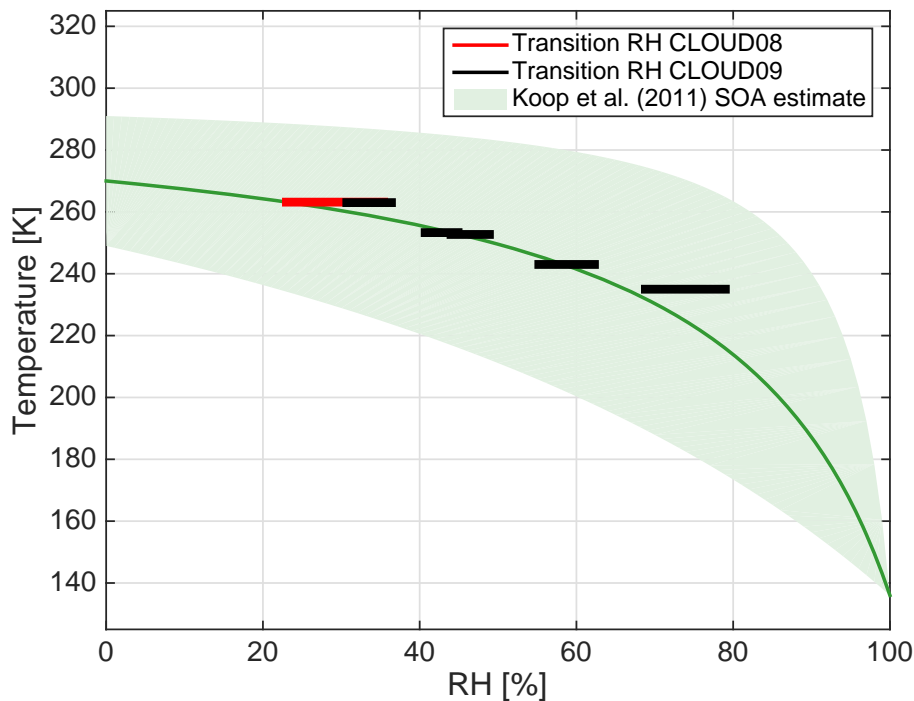


**Figure 11.** Transition RH at different temperatures. The horizontal lines show the RH range for the transition and the the width of the lines represent the temperature uncertainty of 2 K. The green curve is the generic SOA estimate from Koop et al. (2011) and the shaded area represents the upper and lower boundary for the estimate.

[Title Page](#)
[Abstract](#)
[Introduction](#)
[Conclusions](#)
[References](#)
[Tables](#)
[Figures](#)
[◀](#)
[▶](#)
[◀](#)
[▶](#)
[Back](#)
[Close](#)
[Full Screen / Esc](#)
[Printer-friendly Version](#)
[Interactive Discussion](#)
